Supplementary Materials

Within- and Cross-Participant Classifiers Reveal Different Neural Coding of Information

John A. Clithero, David V. Smith, R. McKell Carter, and Scott A. Huettel

Supplementary Information

Stimuli

Social reward images were cropped to show only the face and were resized to uniform dimensions. Before the main fMRI study, a large set of photographs of young-adult females ($n > 2000$) were rated for attractiveness (on a 10-point scale) by a cohort of heterosexual young-adult males ($n = 16$) who did not participate in subsequent studies. To remove individual bias in the use of the response scale, ratings were normalized by converting to z-scores for each participant and then averaged across all raters. We excluded from our stimulus set 83 photographs whose variability across raters was more than two standard deviations above the average for all photographs. Each participant saw approximately 124 randomly-selected faces while in the scanner, meaning participants did not see any face more than once and participants did not see the same subset of faces.

Monetary rewards were shown as images of the front of United States currency ($1 and $5 bills). Positive monetary amounts were shown in green, and negative monetary amounts were shown in red.

General Linear Model Analyses

As a check on some of our classification results, we also ran a simple general linear model (GLM) in FSL. Statistical analyses were conducted in three stages using the FSL analysis package (Smith et al., 2004). Preprocessed functional data were analyzed using a general linear model with local auto-

correlation correction (Woolrich et al., 2001). For each run, we constructed models comprising 8 regressors corresponding to the amount of the monetary reward ($\$5, \$1, -\$1$, and $-\$5$) and the attractiveness of the facial reward (1-star, 2-star, 3-star, 4-star). A nuisance regressor modeled the target-detection component of each task. Additionally, for the cued trials, we included two additional nuisance regressors that modeled the onset of the cue (one for faces and one for money). All regressors modeled the duration of the event and were convolved with a canonical hemodynamic response function. Our key contrasts involved bidirectional comparisons of all face and monetary stimuli. We then combined data across runs of cued and uncued trials, for each subject, using a fixed-effects model, and combined data across subjects using a mixed-effects model (Beckmann et al., 2003; Woolrich et al., 2004).

All z-statistic images were thresholded using $z > 2.3$ and a corrected cluster-significance threshold of $p < 0.05$ (Worsley, 2001). Statistical overlay images were created using MRIcron (Rorden et al., 2007) and anatomical labels for local maxima were obtained from the Talairach Client (Lancaster et al., 2000). All coordinates for FSL output are reported in MNI space.

General Linear Model Results

We used the GLM approach to identify regions whose relative overall activation differed between reward types (cluster peaks for each of the two main contrasts are listed in **Table S2** and **Table S3**). Next, we evaluated whether there were any significant effects of cuing upon value-related responses at reward delivery. For the two contrasts of interest, we found no significant differences between uncued and cued trials in any brain region, even at a liberal statistical threshold ($p < 0.001$, uncorrected). Therefore, we do not anticipate any confounds when collapsing the functional data across these two tasks.

We also introduced each participant's proportion of exchanges in the exchange task as a covariate in the cross-participants GLM analysis. The difference between experienced monetary rewards and experienced social rewards was positively correlated with exchange rate in several prefrontal regions (**Table S4**), although none in the more ventral parts of medial prefrontal cortex, as was found in the decoding multivariate analyses.

References

Beckmann, C.F., Jenkinson, M., Smith, S.M., 2003. General multilevel linear modeling for group analysis in FMRI. NeuroImage 20, 1052-1063.

Lancaster, J.L., Woldorff, M.G., Parsons, L.M., Liotti, M., Freitas, C.S., Rainey, L., Kochunov, P.V., Nickerson, D., Mikiten, S.A., Fox, P.T., 2000. Automated Talairach atlas labels for functional brain mapping. Human Brain Mapping 10, 120-131.

Rorden, C., Karnath, H.O., Bonilha, L., 2007. Improving lesion-symptom mapping. Journal of Cognitive Neuroscience 19, 1081-1088.

Smith, S.M., Jenkinson, M., Woolrich, M.W., Beckmann, C.F., Behrens, T.E.J., Johansen-Berg, H., Bannister, P.R., De Luca, M., Drobnjak, I., Flitney, D.E., Niazy, R.K., Saunders, J., Vickers, J., Zhang, Y.Y., De Stefano, N., Brady, J.M., Matthews, P.M., 2004. Advances in functional and structural MR image analysis and implementation as FSL. NeuroImage 23, S208-S219.

Woolrich, M.W., Ripley, B.D., Brady, M., Smith, S.M., 2001. Temporal autocorrelation in univariate linear modeling of FMRI data. NeuroImage 14, 1370-1386.

Woolrich, M.W., Behrens, T.E., Beckmann, C.F., Jenkinson, M., Smith, S.M., 2004. Multilevel linear modelling for FMRI group analysis using Bayesian inference. NeuroImage 21, 1732-1747.

Worsley, K.J., 2001. Statistical analysis of activation images. In: Jezzard, P., Matthews, P.M., Smith, S.M. (Eds.), Functional MRI: An Introduction to Methods. Oxford University Press, USA.

Supplementary Figures

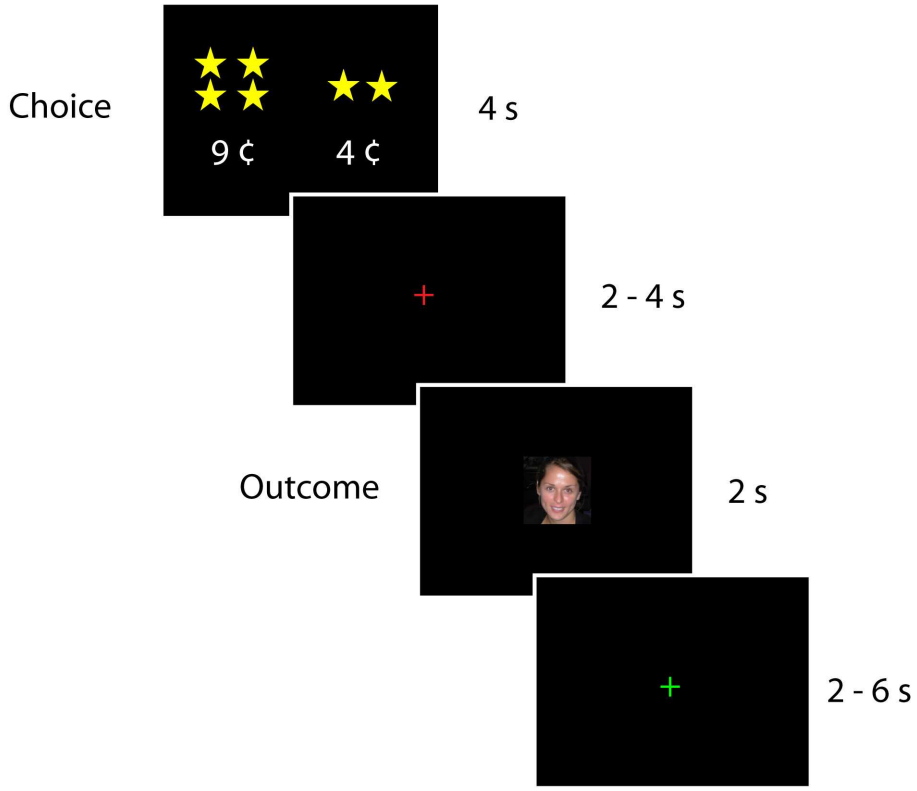

Figure S1: *Exchange Task*. Participants also completed an economic exchange task. On each trial, the participant chose whether to spend more money to view a more attractive face or less money to view a less attractive face. After the 4 s allocated for the choice between seeing faces of different rating (here, 2 or 4 stars) and a 2 - 4 s variable interval, a single face was randomly selected from the chosen attractiveness category (1 to 4 stars) and displayed for 2 s. Trials were separated by a variable ITI of 2 - 6 s.

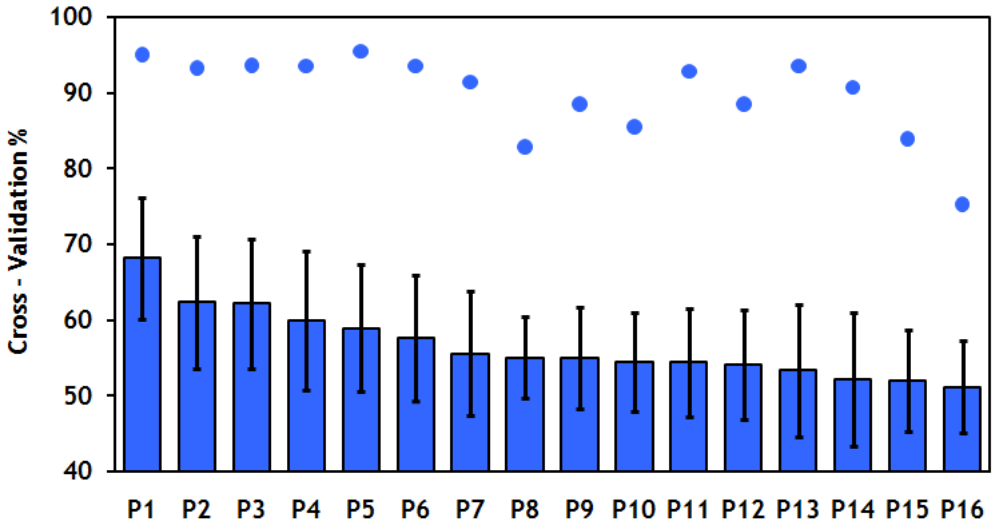

Figure S2: *Individual participant cross-validation summary*. The average cross-validation (CV) percentage for each participant across all 27012 searchlights is plotted, with error bars representing that participant's standard deviation. The global maximum CV for each subject is plotted in dots. Participants are presented in descending order based on average CV.

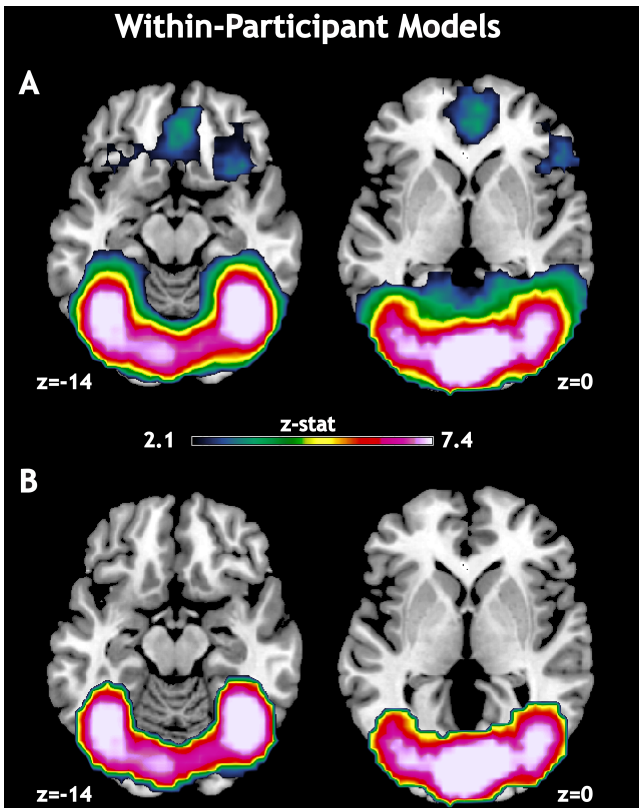

Figure S3: *Statistical thresholding for within-participant decoding analysis*. A whole-brain map of p values from the binomial test was created and then subjected to two different significance thresholds. These are the same slices shown in **Figure 2A**. Higher z-scores correspond to higher cross-validation percentages. **(A)** Threshold for significance was determined using false discovery rate (FDR) of 5%. This correction determined that 10300 voxels in the whole-brain mask had cross-validation rates that were significantly above chance (50%). **(B)** Threshold for significance was determined using a full Bonferroni correction for $p < 0.05$. This correction determined that 2559 voxels in the whole-brain mask had cross-validation rates that were significantly above chance (50%).

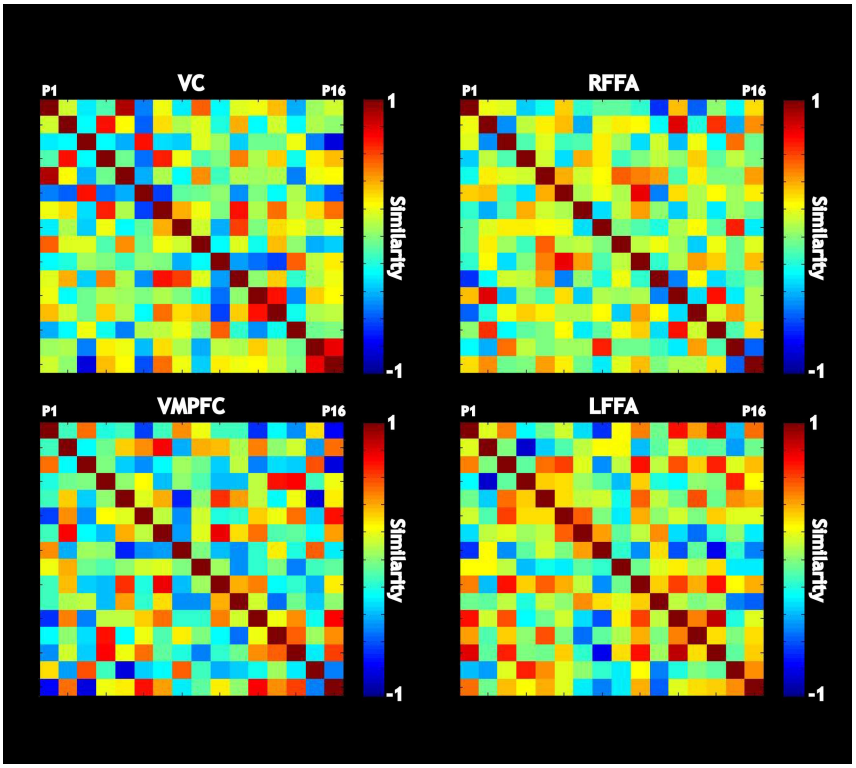

Figure S4: *Cross-participant ROI similarity matrices indicate different information weighting*. Using the ten voxels from the local maxima searchlights with the greatest average absolute weight, we computed similarity (using Pearson correlation) between participants for those ten voxels. The ROIs were visual cortex (VC), left fusiform face area (LFFA), right fusiform face area (RFFA), and ventromedial prefrontal cortex (VMPFC). A measure of 1 represents perfect similarity and -1 represents perfect dissimilarity. Although VC, RFFA, and VMPFC were used in the main paper (**Figure 4**), we include LFFA for completeness. Second-order similarities are listed in **Table S1**.

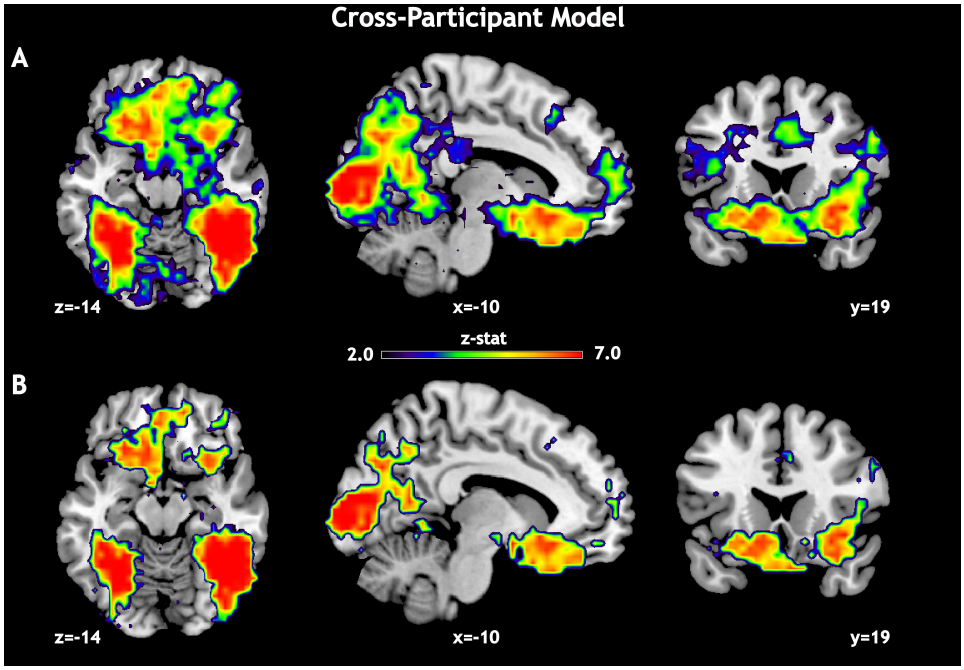

Figure S5: *Statistical thresholding for cross-participant decoding analysis*. A whole-brain map of p values from the binomial test on the cross-participant model was created and then subjected to two different significance thresholds. These are the same slices shown in **Figure 5**. Higher z-scores correspond to higher cross-validation percentages. **(A)** Threshold for significance was determined using false discovery rate (FDR) of 5%. This correction determined that 12698 voxels in the whole-brain mask had cross-validation rates that were significantly above chance (50%). **(B)** Threshold for significance was determined using a full Bonferroni correction for $p < 0.05$. This correction determined that 4343 voxels in the whole-brain mask had cross-validation rates that were significantly above chance (50%).

Supplementary Tables

Table S1: Second-Order Cross-ROI Similarity.

ROI	LFFA	RFFA	VC	VMPFC
LFFA	1	0.14	-0.08	-0.11
RFFA		1	-0.18	0.26
VC			1	0.11
VMPFC				1

Table S2: *General Linear Model Results. Money > Face Contrast.* Cluster maxima are listed in bold.

x	y	z	Region	BA	z-stat
34	-54	40	Inferior Parietal Lobule	40	**5.46**
-8	-76	6	Cuneus	23	5.32
-8	-72	8	Posterior Cingulate	30	5.2
36	-66	40	Inferior Parietal Lobule	39	5.01
-2	-86	10	Cuneus	17	5
-8	-86	6	Cuneus	17	5
46	12	46	Middle Frontal Gyrus	8	**5**
34	12	46	Middle Frontal Gyrus	6	4.7
40	38	34	Superior Frontal Gyrus	9	4.67
46	38	30	Middle Frontal Gyrus	46	4.56
34	6	50	Middle Frontal Gyrus	6	4.51
2	20	42	Cingulate Gyrus	32	4.43
-46	6	46	Middle Frontal Gyrus	8	3.89
-46	38	22	Middle Frontal Gyrus	46	**3.89**
-44	12	40	Middle Frontal Gyrus	9	3.8
-46	4	52	Middle Frontal Gyrus	6	3.66
-50	18	32	Middle Frontal Gyrus	9	3.6
-44	14	32	Middle Frontal Gyrus	9	3.54
54	-46	-10	Middle Temporal Gyrus	37	**3.75**
66	-28	-12	Middle Temporal Gyrus	21	3.67
44	-34	-4	Superior Temporal Gyrus	22	3.52
52	-54	-8	Inferior Temporal Gyrus	37	3.51
56	-42	-18	Middle Temporal Gyrus	20	3.21
62	-38	-16	Middle Temporal Gyrus	21	3.1

Table S3: *General Linear Model Results. Face > Money Contrast.* Cluster maxima are listed in bold.

x	y	z	Region	BA	z-stat
48	-68	-6	Inferior Temporal Gyrus	37	**4.66**
36	-50	-18	Fusiform Gyrus	37	4.52
52	-68	6	Middle Temporal Gyrus	37	4.31
48	-74	4	Middle Occipital Gyrus	19	4.3
42	-86	-4	Inferior Occipital Gyrus	18	4.12
42	-52	-20	Fusiform Gyrus	37	4.04
6	46	-16	Medial Frontal Gyrus	11	**4.74**
-2	36	-16	Medial Frontal Gyrus	11	4.18
38	32	-22	Inferior Frontal Gyrus	47	4.08
6	52	-8	Medial Frontal Gyrus	10	3.91
-6	20	-14	Subcallosal Gyrus	25	3.62
-6	54	-4	Medial Frontal Gyrus	10	3.27
-38	-54	-20	Fusiform Gyrus	37	**4.89**
-30	-12	-12	Parahippocampal Gyrus	Hippocampus	3.57
-32	-20	-16	Parahippocampal Gyrus	Hippocampus	3.49
-36	-38	-18	Fusiform Gyrus	37	3.29
-50	-68	14	Middle Temporal Gyrus	19	**4.9**
-48	-78	78	Middle Temporal Gyrus	39	4.62
-38	-84	-4	Inferior Occipital Gyrus	19	4.49
-54	-62	26	Superior Temporal Gyrus	39	3
-44	-64	28	Middle Temporal Gyrus	39	2.51
-42	36	-18	Middle Frontal Gyrus	11	**3.29**
-42	36	-22	Inferior Frontal Gyrus	47	3.28
-24	26	-14	Inferior Frontal Gyrus	11	3.26
-34	34	-22	Inferior Frontal Gyrus	47	3.23
-34	30	-20	Inferior Frontal Gyrus	47	3.22
-36	24	-24	Superior Temporal Gyrus	38	3.17

Table S4: *General Linear Model Results. Exchange Task as Covariate for Money > Face Contrast*. Cluster maxima are listed in bold.

x	y	z	Region	BA	z-stat
18	48	44	Superior Frontal Gyrus	8	**3.67**
10	68	22	Superior Frontal Gyrus	10	3.42
8	62	34	Superior Frontal Gyrus	9	3.38
6	66	20	Medial Frontal Gyrus	10	3.25
18	64	26	Superior Frontal Gyrus	10	3.25
36	34	32	Middle Frontal Gyrus	9	3.02